MULTISTAGE DECODING-AIDED CHANNEL ESTIMATION AND EQUALIZATION FOR DVB-H IN SINGLE-FREQUENCY NETWORKS

Mario Poggioni, Luca Rugini and Paolo Banelli

DIEI, University of Perugia, Via G. Duranti 93, 06125 Perugia, Italy

ABSTRACT

In single-frequency network (SFN) broadcasting systems, the presence of several transmitters translates into an equivalent channel with relevant sparsity in the delay domain, which may significantly impair the error performance. In DVB-H systems this channel sparsity, coupled with the time variation due to mobile users, renders the channel estimation task very challenging, especially when only a moderate complexity is tolerated at the receiver side. To solve this problem, this work proposes a new low-complexity multistage channel estimation technique that exploits the data at the output of the channel decoder, as well as a simple parallel intercarrier interference (ICI) canceller. The proposed scheme iteratively estimates data and channel in a joint fashion, and also includes a regularization-based preprocessing stage to specially deal with severe channel sparsity. Simulation results show that our low-complexity scheme is adequate for practical implementations of fast-mobility DVB-H receivers in all SFN scenarios.

Index Terms— Channel estimation, ICI cancellation, SFN, DVB-T/H, coded OFDM, Doppler spread, fast fading channels.

1. INTRODUCTION

A single-frequency network (SFN) is a broadcast network characterized by the presence of two or more transmitters that make use of the same spectrum to broadcast a unique signal. Despite their advantages, SFNs constitute a serious challenge for the receiver design of mobile users, because the presence of both severe multipath and fast fading makes the channel estimation and equalization especially difficult. In this work, we aim to find *low-complexity* solutions, which can be practically applied in handheld DVB-H receivers [1].

To this end, we employ time-invariant (TI) channel estimation approaches, which turn out to be also useful in many time-varying (TV) scenarios. However, TI channel estimation alone can be ineffective in fast TV channels, because the block-fading approximation (i.e., with a TI frequency response within each OFDM block) actually leads to the estimation of only the average channel impulse response (CIR) in each block. Therefore, it is necessary to resort to TV channel estimation techniques, characterized by higher complexity. For instance, several efforts have been recently documented in the OFDM literature to reduce the problem of a TV channel estimation to the estimation of a reduced number of parameters [2]. Most of these methods are captured by the concept of basis expansion model (BEM) for TV channels. Unfortunately, the specific channel structure of SFNs makes it difficult to estimate the BEM coefficients, since this problem is highly ill-conditioned [3]. Therefore, we propose to resort to regularization techniques jointly with ad-hoc solutions, which also exploit a non-uniform channel sampling technique. We show that it is also necessary to employ an iterative approach to boost the channel estimation and enhance the overall DVB-H BER performance, through the cancellation of the intercarrier interference (ICI) arising in fast TV channels.

In order to deploy low-complexity solutions, we employ the BEM only to obtain a first rough estimate of the channel. Successively, we refine our first estimation by means of very simple TV channel estimation techniques, with a complexity similar to TI techniques [4], by exploiting the presence of a forward error correcting code (FEC) (convolutional code) and by resorting to an iterative approach to improve the performance, following the philosophy of [5]. A further improvement is obtained by taking into account the channel state information (CSI), obtained from the channel estimation, inside the convolutional decoder. Finally, for the ICI mitigation we consider a simple ICI cancellation on each subcarrier, which exploits channel coding to better estimate the interfering data. The good BER performance, shown by simulation results, suggests that this work can be useful to enhance the receiving capability in current DVB-H systems.

2. SYSTEM MODEL

We consider an SFN system with two DVB-H transmitters/repeaters. The equivalent channel model is described in the next subsection.

2.1. SFN Channel Model

The presence of two transmitters induces at the receiver a two components (discrete-time) channel $\mathbf{h}_T[k] = \mathbf{h}_1^{(L,0)}[k] + \mathbf{h}_2^{(L,\Delta_{12})}[k]$, where the wireless channels $\mathbf{h}_i[k], i = 1, 2$, between each transmitter and the receiver are typically separated by a certain delay $\Delta_{12}T_S$, as expressed by

$$\mathbf{h}_1^{(L,0)}[k] = \begin{bmatrix} \mathbf{h}_1[k] \\ \mathbf{0}_{(L-L_1)\times 1} \end{bmatrix}; \mathbf{h}_2^{(L,\Delta_{12})}[k] = \begin{bmatrix} \mathbf{0}_{\Delta_{12}\times 1} \\ \mathbf{h}_2[k] \end{bmatrix}, \quad (1)$$

where L is the total number of taps of $\mathbf{h}_T[k]$, including the effect of the delay, L_i is the number of taps of $\mathbf{h}_i[k]$, T_S is the sampling time, and k is the sampling time index.

We model each path in $\mathbf{h}_i[k]$ as a wide-sense stationary with uncorrelated scattering (WSSUS) process, compliant with the COST 207 standard [6]. Specifically, we consider, for each continuous-time channel $h_{i,c}(t, \tau), i = 1, 2$, the Typical Urban (TU) power-delay profile. This results in an L-taps discrete-time model, where $h_l[k] = [\mathbf{h}_T[k]]_l$ can be written as

$$h_l[k] = h_{1,l}^{(L,0)}[k] + h_{2,l}^{(L,\Delta_{12})}[k] = h_{1,c}^{(L,0)}(kT_S, lT_S) + h_{2,c}^{(L,\Delta_{12})}(kT_S, lT_S), l = 0, ..., L-1. \quad (2)$$

Note that $L = \Delta_{12} + L_2$, where in TU channels $L_2 = L_1 = 64$ [6]. Typically, $\Delta_{12} \gg L_1$, such that each tap $h_l[k]$ of $\mathbf{h}[k]$ seen by the receiver comes from a single channel component (see Figure 1), because the other one is zero, as expressed by

$$h_l[k] = \begin{cases} h_{1,l}[k], & 0 \le l \le L_1, \\ 0, & L_1 < l < \Delta_{12}, \\ h_{2,l-\Delta_{12}}[k], & \Delta_{12} \le l \le \Delta_{12} + L_2. \end{cases} \quad (3)$$

978-1-4244-3696-5/09/$25.00 © 2009 IEEE

2.2. OFDM System Model

We assume $L_{CP} \geq L$, i.e., there is no interblock interference (IBI) [7]. The OFDM system in the frequency domain can be represented, for the mth OFDM block, as

$$\mathbf{y}^{(m)} = \mathbf{H}_F^{(m)}\mathbf{s}^{(m)} + \mathbf{n}^{(m)}, \quad (4)$$

where $\mathbf{y}^{(m)}$, is the received signal vector, with size equal to the number N of subcarriers, $\mathbf{s}^{(m)} = \mathbf{d}^{(m)} + \mathbf{p}_s^{(m)} + \mathbf{p}_c^{(m)}$ is the transmitted signal vector, which contains the frequency-domain multiplexed data $\mathbf{d}^{(m)}$, scattered pilots $\mathbf{p}_s^{(m)}$, and continuous pilots $\mathbf{p}_c^{(m)}$ [1], and $\mathbf{n}^{(m)}$ is the noise vector. Moreover,

$$\mathbf{H}_F^{(m)} = \mathbf{F}_N \mathbf{H}_T^{(m)} \mathbf{F}_N^H \quad (5)$$

is the frequency-domain channel matrix, $\mathbf{H}_T^{(m)}$ is the time-domain matrix that, after CP removal, contains on its $(l+1)$th diagonal the time evolution $h_l^{(m)}[k] = h_l[m(N+L_{CP})+L_{CP}+k]$ of the lth channel tap, and $\mathbf{F}_N$ is the unitary DFT matrix of size N.

In TI channels, $\mathbf{H}_T^{(m)}$ is circulant, so that $\mathbf{H}_F^{(m)}$ is diagonal and contains the DFT of the CIR, as expressed by

$$\mathbf{H}_F^{(m)} = diag(\sqrt{N}\mathbf{F}_N^{(L)}\mathbf{h}_T^{(m)}[k]), \quad (6)$$

where $\mathbf{F}_N^{(L)}$ is the rectangular matrix that selects only the first L columns of $\mathbf{F}_N$ and $\mathbf{h}_T^{(m)}[k] = [h_0^{(m)}[k], ..., h_{L-1}^{(m)}[k]]$ is the CIR, which in TI channel is independent from the time index k. On the contrary, in TV channels, $\mathbf{H}_F^{(m)}$ departs from a diagonal matrix, and off-diagonals contributions, representing the discrete-domain Doppler spread, start to increase as long as the time variation of the channel increases, inducing on each transmitted data the so-called ICI [8][9]. In this case, the main diagonal of $\mathbf{H}_F^{(m)}$ contains the DFT of the average CIR in the mth block.

3. MULTISTAGE CHANNEL ESTIMATION AND EQUALIZATION

In order to counteract both sparsity and ICI, we propose a modular algorithm based on a multistage approach. Each stage is devoted to a specific task, such as channel estimation, equalization, or ICI cancellation. Since low complexity is our main constraint, each stage should be as simple as possible, so that it can be implemented using standard chipsets already available on the market. Performance can then be improved by iterating the algorithm, but preferably using hard decisions rather than soft-decision estimates, which may not be available at the output of standard chipsets.

Our whole algorithm is summarized in Figure 2, where solid lines indicate the main data flow and dotted lines represent the auxiliary data. In the following, we describe the main stages, motivating the choices we have made.

3.1. BEM-based TV Channel Estimation

We focus on the BEM, firstly presented by Bello [10] and fully developed in [2]. First, we reconstruct the time variability of the channel over multiple OFDM blocks, and successively we average the TV estimated channel over the block of interest only. This results in a better average CIR estimation with respect to algorithms based on the single OFDM block of interest.

Specifically, we adapt the multiblock BEM approach proposed in [11] to the present scenario, where the time evolution of the channel taps during $2J+1$ OFDM blocks is approximated as

$$\mathbf{h}_{vec} \cong (\mathbf{B} \otimes \mathbf{I}_L)\,\mathbf{h}, \quad (7)$$

where $\otimes$ is the Kronecker product, $\mathbf{h}_{vec}$ is a $(2J+1)N(Q+1)(L_1+L_2)$ vector expressed by

$$\mathbf{h}_{vec} = vec(\tilde{\mathbf{H}}_T^{(m-J)}, ..., \tilde{\mathbf{H}}_T^{(m+J)}), \quad (8)$$

$\tilde{\mathbf{H}}_T^{(m)} = [\mathbf{h}_T^{(m)}[0], ..., \mathbf{h}_T^{(m)}[N-1]]^T$, $\mathbf{B} = [\mathbf{b}_0, ..., \mathbf{b}_Q]$ is the matrix that collects the $Q+1$ basis functions and $\mathbf{h} = [\mathbf{h}_1^T ... \mathbf{h}_Q^T]^T$ is the vector that collects the $(Q+1)(L_1+L_2)$ BEM coefficients for all the L_1+L_2 non-zero taps, whose estimation is the goal of this subsection. We employ orthogonal polynomial basis functions, which are suitable for low-to-medium time variability. We also assume a perfect knowledge of the taps positions, which, for instance, can be obtained by means of energy detectors or matching pursuit algorithms [12]. We express the observation vector $\mathbf{y}_p$, extracted from (4) using only the elements that correspond to the pilot positions, from block $m-J$ to block $m+J$ as

$$\mathbf{y}_p = \mathbf{P}(\mathbf{p}_m)\mathbf{h} + \mathbf{i}_p + \mathbf{n}_p, \quad (9)$$

where $\mathbf{y}_p = [(\mathbf{y}_p^{(m-J)})^T, ..., (\mathbf{y}_p^{(m+J)})^T]^T$, $\mathbf{p}_m = [(\mathbf{p}^{(m-J)})^T, ..., (\mathbf{p}^{(m+J)})^T]^T$, $\mathbf{p}^{(m)}$ is the pilot vector for the mth block, $\mathbf{i}_p$ is the ICI vector induced by the data and by those pilots not used in the channel estimation, and $\mathbf{n}_p$ is the noise vector. Moreover, $\mathbf{P}(\mathbf{p}_m) = [\overline{\mathbf{P}}^T(\mathbf{p}^{(m-J)}), ..., \overline{\mathbf{P}}^T(\mathbf{p}^{(m+J)})]^T$, where $\overline{\mathbf{P}}(\mathbf{p}^{(m)})$ represents a known matrix for the mth block, expressed as

$$\overline{\mathbf{P}}(\mathbf{p}^{(m)}) = [\ \mathbf{D}_0^{(p)}(m) \quad ..., \quad \mathbf{D}_Q^{(p)}(m)\ ] \\ (\mathbf{I}_{Q+1} \otimes Diag(\mathbf{s}^{(p)}(m))\mathbf{F}^{(L)}(\mathbf{p}^{(m)})), \quad (10)$$

where $\mathbf{s}^{(p)}(m)$ is the vector containing the non-zero values of $\mathbf{p}^{(m)}$,

$$\mathbf{D}_q^{(p)}(m) = \mathbf{F}^{(L)}(\mathbf{p}^{(m)}) Diag\left\{\mathbf{b}_q^{(m)}\right\}\left(\mathbf{F}^{(L)}(\mathbf{p}^{(m)})\right)^H, \quad (11)$$

where $\mathbf{F}^{(L)}(\mathbf{p}^{(m)})$ is the submatrix of $\mathbf{F}_N^{(L)}$ containing only the rows corresponding to the pilot positions of $\mathbf{p}^{(m)}$, and $\mathbf{b}_q^{(m)}$ is the subvector of $\mathbf{b}_q$ relative to the mth block.

The BEM coefficients are simply obtained by least squares (LS) estimation,

$$\hat{\mathbf{h}} = \mathbf{P}^{\dagger}(\mathbf{p}_m)\mathbf{y}_p, \quad (12)$$

where $\mathbf{P}^{\dagger} = (\mathbf{P}^H\mathbf{P})^{-1}\mathbf{P}^H$ is the Moore-Penrose pseudo-inverse of $\mathbf{P}$. The estimated coefficients $\hat{\mathbf{h}}$ are then used to reconstruct the TV CIR, which is averaged over the mth block to obtain the approximate TI CIR.

3.2. Preprocessing to Avoid Aliasing

Usually, low-complexity TI CIR estimation methods for DVB-H only consider $\mathbf{p}^{(m)} = \mathbf{p}_s^{(m)}$, because the scattered pilots have a regular pattern. The received signal corresponding to $\mathbf{P}(\mathbf{p}_m)$ constitutes an *equispaced sampling* (every 12 subcarriers) of the channel in the frequency domain. Thus, due to the Nyquist-Shannon sampling theorem, the signal received on the scattered pilots is characterized, in the delay domain, by CIR replicas separated by $T_R = NT_S/12$ samples. As a consequence, for certain values of Δ_{12}, $LT_S > T_R$, there exists *aliasing* in the delay domain. In most cases, it is possible to exploit the channel sparsity by means of *undersampling* techniques, as shown in Figure 1, since the aliased CIR does not overlap with the true CIR. However, when the aliased CIR overlaps, $\mathbf{P}(\mathbf{p}_m)$ is usually very ill-conditioned, with condition number up to the order of 10^{16}, leading to completely useless estimates. This extremely-high condition number also impairs the correct use of standard regularization techniques, such as ridge regression, truncated singular

value decomposition (TSVD), conjugate gradient, column weighting, LSQI, [3], which do not help when the condition number is so high.

To reduce the condition number, we are forced to use some specific techniques. First, in the BEM channel estimation, we choose $J = 1$, instead of the more common choice $J = 0$, and we use *all* the pilots that are available for DVB-H, i.e., $\mathbf{p}^{(m)} = \mathbf{p}_s^{(m)} + \mathbf{p}_c^{(m)}$. This reduces the condition number to ≈ 200, which enables the use of regularization techniques, such as the TSVD [3], which we focus on. Consequently, in (12), $\mathbf{P}^{\dagger}(\mathbf{p}_m)$ is replaced by

$$\mathbf{T} = \mathbf{V}\hat{\mathbf{S}}_{k_T}^{\dagger}\mathbf{U}^H, \tag{13}$$

where $\mathbf{P}(\mathbf{p}_m) = \mathbf{USV}^H$, and $\hat{\mathbf{S}}_{k_T}$ is equal to $\mathbf{S}$ in the first k_T diagonal elements only, while the others are set to zero. Although the SVD of a large matrix (e.g., 480×2651) may appear as very complex, due to the pilot arrangement of DVB-H [1], $\mathbf{P}(\mathbf{p}_m) = \mathbf{P}(\mathbf{p}_{m+4})$, and hence only four matrices are requested, which can be precomputed and stored.

3.3. First Equalization

After the regularization-based BEM channel estimation, the frequency-domain channel matrix in the mth block could be reconstructed as

$$\bar{\mathbf{H}}_F^{(m)} = \sum_{q=0}^{Q} circ(\sqrt{N}\mathbf{F}_N\mathbf{b}_q^{(m)})diag\left(\mathbf{F}_N^{(L)}\hat{\mathbf{h}}_q\right)$$

$$= Diag(\bar{\mathbf{\Lambda}}_{0(m)}^{(f)}) + \sum_{q=1}^{Q} circ(\sqrt{N}\mathbf{F}_N\mathbf{b}_q^{(m)})diag\left(\mathbf{F}_N^{(L)}\hat{\mathbf{h}}_q\right), \tag{14}$$

where $\mathbf{A} = circ(\mathbf{a})$ is the circulant matrix with $\mathbf{a}$ in its first column, the subvector $\hat{\mathbf{h}}_q$ of $\hat{\mathbf{h}}$ is the estimate of $\mathbf{h}_q$, and $\bar{\mathbf{\Lambda}}_{0(m)}^{(f)} = diag(\bar{\mathbf{H}}_F^{(m)})$ represents the DFT of the estimated average CIR. However, equalization methods based on the direct use of the whole estimated channel matrix present two drawbacks. First, TV equalization methods such as [8] and [9], which are generally considered as low-complexity techniques, are too complicated for our purposes. Second, our simplified channel estimation is adequate for TI average CIR estimation, but the estimation of the time variation is not very accurate for TV equalization. Therefore, we use only $\bar{\mathbf{\Lambda}}_{0(m)}^{(f)}$ to perform a TI per-subcarrier channel equalization:

$$[\bar{\mathbf{s}}_{TI}^{(m)}]_k = [\mathbf{y}^{(m)}]_k / [\bar{\mathbf{\Lambda}}_{0(m)}^{(f)}]_k, \forall k = 1, ..., N. \tag{15}$$

However, to improve performance, we refine this first estimate by resorting to an *iterative* strategy, which is discussed below.

3.4. Iterative Approach Based on Re-Encoding

In order to boost performance, we aim at improving the quality of the channel estimate. We choose a joint channel and data estimation with limited complexity, aided by the output of a convolutional decoder, with a philosophy similar to [5]. After Viterbi decoding with input $\bar{\mathbf{s}}_{TI}^{(m)}$, we subsequently re-encode the data obtaining a new estimate $\bar{\mathbf{s}}_{CC}^{(m)}$.

We can then use the re-encoded data as *virtual* pilots, to be used for channel estimation. Indeed, by selecting as virtual pilots those data of $\bar{\mathbf{s}}_{CC}^{(m)}$ that correspond to the positions of the scattered pilots in the $(m+2)$th block, we obtain a set of new pilots (virtual plus scattered) that are regularly spaced. Since this separation is reduced from 12 to 6 subcarriers, the aliasing problem is highly reduced, and standard techniques can be employed. Specifically, we make use of the channel estimation Method II developed in [4]. Hence, we first perform a simple TI channel estimation on the virtual and scattered pilot subcarriers, as expressed by

$$\tilde{\mathbf{\Lambda}}_{0(m)}^{(f)} = \mathbf{\Sigma}Diag(\mathbf{p}_v^{(m)} + \mathbf{p}_s^{(m)})^{\dagger}\mathbf{y}^{(m)}, \tag{16}$$

where $\mathbf{\Sigma}$ is a selection matrix that extracts only the elements related to the (virtual and scattered) pilot subcarriers. Second, we perform a Nyquist cardinal interpolation to estimate the channel $\hat{\mathbf{\Lambda}}_{0(m)}^{(f)}$ also on the other subcarriers, as expressed by

$$\hat{\mathbf{\Lambda}}_{0(m)}^{(f)} = 6\mathbf{F}_N^{(L)}\left(\mathbf{F}^{(L)}(\mathbf{p}_v^{(m)} + \mathbf{p}_s^{(m)})\right)^H \tilde{\mathbf{\Lambda}}_{0(m)}^{(f)}. \tag{17}$$

Third, we perform a TV channel estimation through linear interpolation of the TI estimates $\hat{\mathbf{\Lambda}}_{0(m)}^{(f)}$ of 3 blocks, using those from $m-1$ to $m+1$ [4].

3.5. Parallel ICI Cancellation

By means of Equations 23-27 in [4], we reconstruct the channel matrix $\hat{\mathbf{H}}_F^{(m)}$, which is used together with $\bar{\mathbf{s}}_{CC}^{(m)}$, to cancel the ICI, as expressed by:

$$[\hat{\mathbf{s}}^{(m)}]_k = \left(y_k - \sum_{d=-D, d\neq 0}^{D} [\hat{\mathbf{H}}_F^{(m)}]_{k,d}[\bar{\mathbf{s}}_{CC}^{(m)}]_{k+d}\right) / [\hat{\mathbf{\Lambda}}_{0(m)}^{(f)}]_k, \forall k = 1, ..., N, \tag{18}$$

where D is the number of diagonals subtracted from either side. Finally, we iterate the data-aided TV channel estimation and the parallel ICI cancellation for i additional times, in order to obtain a better refinement of the data estimate. Specifically, after i additional iterations, described in Figure 2, the new quantities $\hat{\mathbf{H}}_{F,i}^{(m)}$, $\bar{\mathbf{s}}_{CC,i}^{(m)}$, and $\hat{\mathbf{\Lambda}}_{0(m),i}^{(f)}$ are available, which can be used like in (18) to cancel out the ICI from y_k, thus obtaining a more accurate data estimate $\hat{\mathbf{s}}_i^{(m)}$.

We highlight that the considered parallel hard cancellation is the simplest method that can mitigate the ICI, since its complexity is linear in both the number N of subcarriers and the number $2D$ of diagonals subtracted. However, if complexity is not an issue, more refined algorithms with complexity $\mathcal{O}(D^2N)$, such as minimum mean-squared error (MMSE) techniques, could be included [8][9]. To further improve performance, at the price of additional complexity, the re-encoding process could benefit from a soft-output Viterbi decoder, so that soft ICI cancellation could be performed. However, due to the low-complexity requirements, these methods are not considered herein.

4. SIMULATION RESULTS

We have simulated a DVB-H 8k system with bandwidth 8 MHz, 16-QAM and CP equal to $1/8$ of the useful symbol duration NT_S. For the convolutional code, we consider the code-rate (CR) $2/3$ [1]. Since the considered channel model is a discrete model, we have approximated the tap delays as integer multiples of the sampling time of the DVB-H (8 MHz), which is $T_S = 7/64\mu$s $\cong 0.109$ μs. The delay Δ_{12} is also approximated as an integer multiple of T_S, in particular by $NT_S/12 \cong 682T_S$. This choice corresponds to the worst case aliasing scenario where the two CIR replicas completely overlap in delay domain, denoted as *total aliasing*. Moreover, in this worst case scenario, we assign the same received power to both the DVB-H signals coming from the two transmitters. The carrier frequency is 800 MHz. We choose two values of Doppler spread: 110 Hz (speed equal to 150 km/h), and 140 Hz (190 km/h). The time

variation of the channel taps is simulated by the sum-of-sinusoids method in [13], leading to the widely used Jakes' Doppler spectrum. At the receiver, the TSVD truncation parameter is $k_T = 445$, and we use $J = 1$ unless otherwise stated. For the parallel ICI cancellation, we choose $D = 8$. A soft-input Viterbi decoder with 4-bit quantization is employed. In our algorithm, we use $i \in \{0, 1, 2\}$ additional iterations.

Figure 3 plots the uncoded BER performance, where we observe similar performance for 110 and 140 Hz Doppler spreads both with the simple TI equalization (after the first rough channel estimation) of (15) and with the genie-aided (GA) case, which refers to a perfect knowledge of $\mathbf{H}_F^{(m)}$ and $\mathbf{s}^{(m)}$ for the ICI cancellation. On the contrary, there is a significant difference in the BER performance after the actual ICI cancellation. This is due to the fact that the CR $2/3$ convolutional code is unable to always correct the errors and it can even worsen the BER: this problem is more evident when the Doppler spread is 140 Hz rather than for 110 Hz. Besides, it is clear that the classical choice $J = 0$ is insufficient to guarantee adequate performance. In addition, it is worth noting in Figure 3 that at low SNR both the ICI cancellation and the iterative procedure worsen the BER performance: this is because, despite the TSVD regularization, the ill-conditioned LS problem enhances the noise, as clearly more evident at low SNR. This behavior can be observed also in Figure 4, where we plot the in-band MSE (i.e., the MSE of the channel estimate $\hat{\mathbf{H}}_{F,i}^{(m)}$, on the $2D + 1$ diagonals used in the ICI cancellation), for each iteration: the MSE is worse at low SNR for high iteration numbers while, obviously, at high SNR the iterative procedure improves the MSE, although this improvement is somewhat limited, especially at 140 Hz Doppler spread.

Figure 5 displays the BER performance counterparts of Figure 3 at the output of the Viterbi decoder. As previously detailed, the Viterbi BER performance at 110 Hz are quite better than at 140 Hz. The exploitation of the CSI provided by the channel estimation can greatly enhance the BER performance. Specifically, in order to preserve a reasonable complexity, we exploit the CSI at the input of the Viterbi decoder, replacing the estimated bit b_j with $\tilde{b}_j = \tan^{-1}\left([\hat{\mathbf{\Lambda}}_{0(m),i}^{(f)}]_k b_j\right)$, where the bit b_j is encoded on a 16-QAM symbol on the kth subcarrier. This way, the metric of the Viterbi decoding is implicitly weighted accordingly to the CSI.

Figure 6 shows that there is a great improvement in the Viterbi BER performance for 110 Hz Doppler, with respect to the corresponding curves of Figure 5, whereas for 140 Hz the performance is similar to Figure 5, because for CR $2/3$ the DVB-H system under examination is still not capable to guarantee acceptable performance. This is due to the fact that, although regularized, the LS problem involved in the channel estimation is still ill-conditioned. Thus, also a very small increase in the ICI power can determine a bad channel estimation for few channel realizations: this fact, however, heavily affects the average BER performance and, in particular, the convolutional code efficacy. This is also the case when CSI is employed.

Finally, we show some BER performance (again exploiting CSI) after the outer Reed-Solomon (RS) decoding at the physical layer, and after the Multiprotocol Encapsulation (MPE) decoding at the data-link layer, where the interleaving matrix has the maximum depth (1024 rows). Figure 7 illustrates the BER after the DVB-H outer code (shortened RS, $(204, 188, t = 8)$) [1], after the first TI equalization, and i additional iterations of the ICI cancellation scheme. Similarly to the Viterbi BER case, there is a notable BER reduction due to the first ICI cancellation, while in the successive iterations the BER is reduced to a lesser extent. On the other hand, Figure 8 shows that, at high SNR, the MPE-FEC at the data-link layer produces a drastically reduced BER after the first ICI cancellation, even though for TI equalization the MPE-FEC is scarcely effective in reducing the BER. If two iterations are employed, the BER is greatly reduced also at low SNR.

5. CONCLUSIONS

In this work we have proposed a low-complexity solution for the channel estimation of a DVB-H system in a SFN. Our solution assessed the issues of fast fading and aliasing in the delay domain, which jointly constitute a serious burden for conventional channel estimation techniques. We have obtained good BER performance without resorting to high-complexity solutions, conversely we have exploited well established techniques, namely BEM, data-aided channel estimation, iterative decoding. This way we make the proposed solution immediately attractive for the market. Future work will assess the system optimization which could further improve the BER performance.

6. REFERENCES

[1] ETSI, "Digital Video Broadcasting (DVB); Framing structure, channel coding and modulation for digital terrestrial television," *ETSI EN 300 744 V1.5.1*, Nov. 2004.

[2] G.B. Giannakis and C. Tepedelenlioglu, "Basis expansion models and diversity techniques for blind identification and equalization of time-varying channels," *Proc. IEEE*, vol. 86, no. 10, pp. 1969–1986, Oct. 1998.

[3] G. H. Golub and C. F. Van Loan, *Matrix Computations*, The Johns Hopkins University Press, 1996.

[4] Y. Mostofi and D.C. Cox, "ICI mitigation for pilot-aided OFDM mobile systems," *IEEE Trans. Wireless Commun.*, vol. 4, no. 2, pp. 765–774, Mar. 2005.

[5] S. Tomasin, A. Gorokhov, H. Yang, and J.-P. Linnartz, "Reduced complexity Doppler compensation for mobile DVB-T," *IEEE PIMRC 2002*, vol. 5, pp. 2077–2081 vol.5, Sept. 2002.

[6] COST 207, "Digital land mobile radio communications," Tech. Rep., European Commission, 1989.

[7] Z. Wang and G.B. Giannakis, "Wireless multicarrier communications," *IEEE Signal Process. Mag.*, vol. 17, no. 3, pp. 29–48, May 2000.

[8] X. Cai and G.B. Giannakis, "Bounding performance and suppressing intercarrier interference in wireless mobile OFDM," *IEEE Trans. Commun.*, vol. 51, no. 12, pp. 2047–2056, Dec. 2003.

[9] P. Schniter, "Low-complexity equalization of OFDM in doubly selective channels," *IEEE Trans. Signal Process.*, vol. 52, no. 4, pp. 1002–1011, Apr. 2004.

[10] P. Bello, "Characterization of randomly time-variant linear channels," *IEEE Trans. Commun. Systems*, vol. 11, no. 4, pp. 360–393, Dec. 1963.

[11] Z. Tang, G. Leus, and P. Banelli, "Pilot-assisted time-varying OFDM channel estimation based on multiple OFDM symbols," *IEEE SPAWC 06*, pp. 1–5, July 2006.

[12] S.F. Cotter, B.D. Rao, K. Engan, and K. Kreutz-Delgado, "Sparse solutions to linear inverse problems with multiple measurement vectors," *IEEE Trans. Signal Process.*, vol. 53, no. 7, pp. 2477–2488, July 2005.

[13] Y.R. Zheng and C. Xiao, "Improved models for the generation of multiple uncorrelated Rayleigh fading waveforms," *IEEE Commun. Lett.*, vol. 6, no. 6, pp. 256–258, Jun 2002.

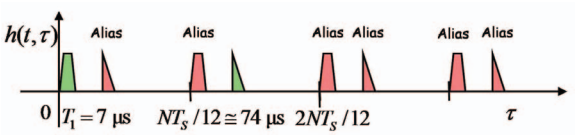

Fig. 1. An example of bandpass sampling in the frequency domain.

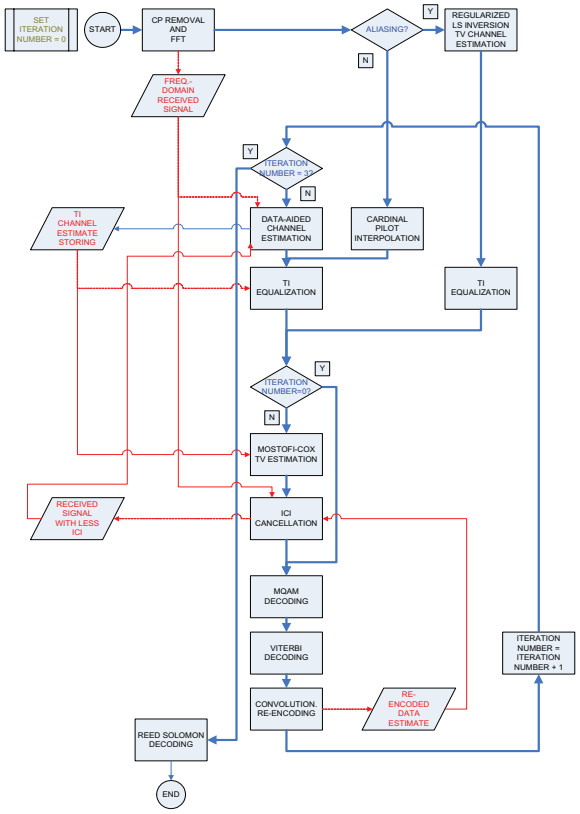

Fig. 2. Decoding algorithm flowchart.

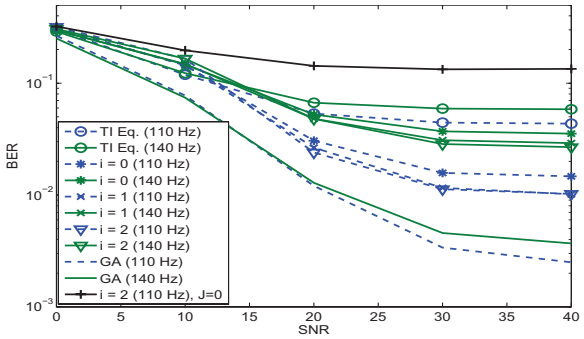

Fig. 3. Uncoded BER performance as a function of the SNR.

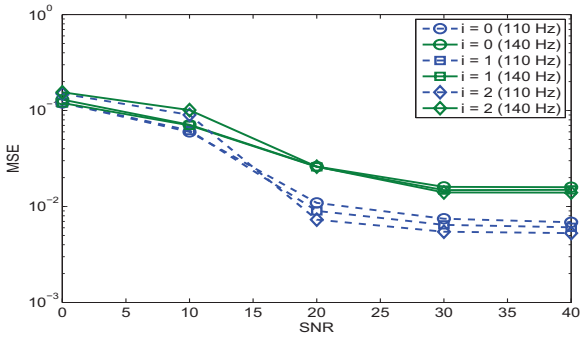

Fig. 4. In-band MSE of the channel estimate.

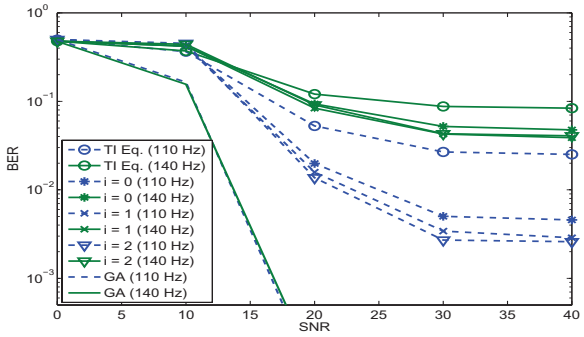

Fig. 5. Coded BER at the output of the conventional Viterbi decoder.

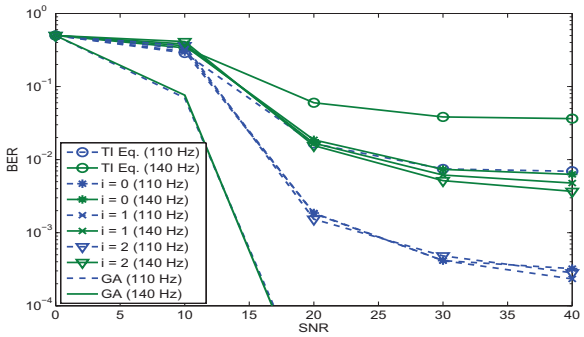

Fig. 6. Coded BER at the output of the CSI-aided Viterbi decoder.

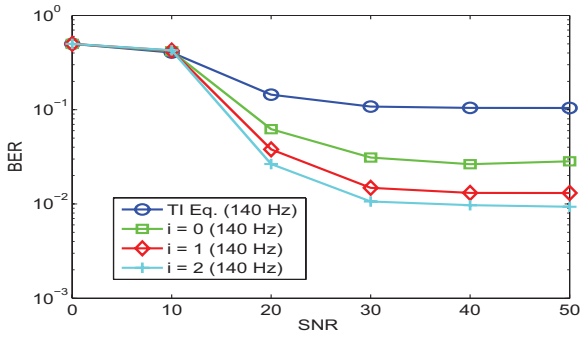

Fig. 7. Coded BER at the output of the outer RS decoder.

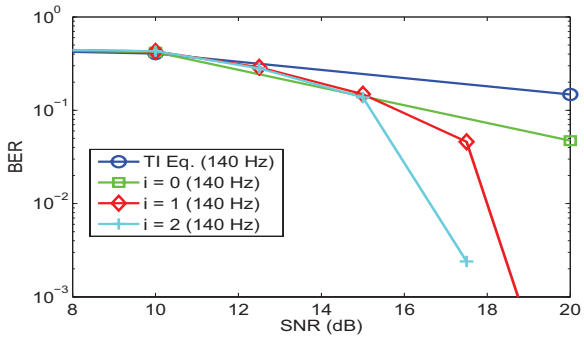

Fig. 8. Data-link layer BER at the output of MPE-FEC decoding.